IOP PUBLISHING JOURNAL OF NEURAL ENGINEERING

J. Neural Eng. **6** (2009) 016006 (16pp) doi:10.1088/1741-2560/6/1/016006

Differential representation of arm movement direction in relation to cortical anatomy and function

Tonio Ball[1,2,5,6], **Andreas Schulze-Bonhage**[1,2], **Ad Aertsen**[2,3] **and Carsten Mehring**[2,4,6]

[1] Epilepsy Center, University Clinic, Albert-Ludwigs-University, 79095 Freiburg, Germany
[2] Bernstein Center for Computational Neuroscience, Albert-Ludwigs-University, 79104 Freiburg, Germany
[3] Neurobiology & Biophysics, Institute for Biology III, Albert-Ludwigs-University, 79104 Freiburg, Germany
[4] Neurobiology & Animal Physiology, Institute for Biology I, Albert-Ludwigs-University, 79104 Freiburg, Germany

Received 28 July 2008
Accepted for publication 16 December 2008
Published 20 January 2009
Online at stacks.iop.org/JNE/6/016006

Abstract

Information about arm movement direction in neuronal activity of the cerebral cortex can be used for movement control mediated by a brain–machine interface (BMI). Here we provide a topographic analysis of the information related to arm movement direction that can be extracted from single trials of electrocorticographic (ECoG) signals recorded from the human frontal and parietal cortex based on a precise assignment of ECoG recording channels to the subjects' individual cortical anatomy and function. To this aim, each electrode contact was identified on structural MRI scans acquired while the electrodes were implanted and was thus related to the brain anatomy of each patient. Cortical function was assessed by direct cortical electrical stimulation. We show that activity from the primary motor cortex, in particular from the region showing hand and arm motor responses upon electrical stimulation, carries most directional information. The premotor, posterior parietal and lateral prefrontal cortex contributed gradually less, but still significant information. This gradient was observed for decoding from movement-related potentials, and from spectral amplitude modulations in low frequencies and in the high gamma band. Our findings thus demonstrate a close topographic correlation between cortical functional anatomy and direction-related information in humans that might be used for brain–machine interfacing.

M This article features online multimedia enhancements

Introduction

Voluntary arm movement in primates involves a network of functionally and structurally distinct areas in the frontal and parietal lobes (Fogassi and Luppino 2005, Geyer *et al* 2000, Hoshi and Tanji 2004). Neuronal activity from these motor areas can be recorded and decoded by implanted brain–machine interfaces (BMIs), allowing for real-time control of external actuators (Carmena *et al* 2003, Chapin *et al* 1999, Hochberg *et al* 2006, Serruya *et al* 2002, Taylor *et al* 2002, Velliste *et al* 2008) and of paralyzed muscles (Moritz *et al* 2008). In animal models, this approach has been developed over the last decade to the point where, today, great efforts are being made toward clinical application of implantable BMIs for the restoration of movement in paralyzed patients. Now,

[5] Address for correspondence: Epilepsy Center, University Clinic Freiburg, Breisacherstr. 64, 79106, Freiburg, Germany.
[6] These authors contributed equally to this work.

at the transition to human application, pre-eminent issues that need to be resolved are as follows: from where in the human motor system signals should be recorded and which recording techniques are most favorable in terms of BMI efficacy and patient safety. Dedicated studies in humans are needed to resolve these questions. For instance, the recording techniques favored in BMI-related animal experiments (e.g. sharp-tipped intra-cortical electrodes) may not be optimal for human clinical application. Furthermore, although different cortical motor areas (Carmena *et al* 2003, Hatsopoulos *et al* 2004, Musallam *et al* 2004, Santucci *et al* 2005, Wessberg *et al* 2000) and signal components (Rickert *et al* 2005) have previously been compared with respect to movement decoding efficiency in monkey experiments, it is not clear to what extent these results can be transferred to interfacing of the human motor system. Therefore, in the present study, we investigated the accuracy of arm movement direction inference based on electrocorticographic (ECoG) signals from the human frontal cortex.

It has been proposed that the ECoG is an excellent BMI modality for human use (Ball *et al* 2004, Leuthardt *et al* 2004, Levine *et al* 2000, Mehring *et al* 2004, Schalk *et al* 2008), as ECoG may offer an optimal compromise between low invasiveness and high information transfer capacity: on the one hand, no disruption of neuronal tissue is required, in contrast to recordings using sharp-tipped intracortical electrodes. On the other hand, compared to the electroencephalogram (EEG), which was proposed as a non-invasive BMI modality (Birbaumer *et al* 1999, Pfurtscheller *et al* 1995, Wolpaw and McFarland 2004), ECoG recordings have a better spatial resolution, a higher signal-to-noise ratio and are less prone to artifact contamination (Ball *et al* 2009, Lachaux *et al* 2003). The ECoG in humans is well established in clinical practice for pre-neurosurgical diagnostics for localizing the seizure onset zone before epilepsy surgery (Engel *et al* 2005, Nair *et al* 2008). For this purpose, strips or arrays of multiple electrodes, each a few mm in diameter, are subdurally implanted, contacting and recording from the cortical brain surface.

A representation of arm movement parameters in trial-averaged ECoG data was initially reported by Toro *et al* (1994) for the alpha frequency range of the ECoG where spatial patterns were modulated by amplitude and to a lesser extent also by the direction of arm movements. More recent studies have shown that information about two-dimensional hand movements as well as individual finger movements can be extracted from single-trial ECoG data (Ball *et al* 2004, Leuthardt *et al* 2004, 2006, Mehring *et al* 2004, Schalk *et al* 2007). The precise distribution of directional information in the ECoG across the anatomical subdivisions of the lateral frontal lobe in individual subjects and also the relation of directional information to individual cortical function as assessed by direct cortical stimulation mapping are, however, not yet clear.

In the present study, we therefore addressed the following questions, based on anatomical and functional characterization of the individual ECoG recording sites (Ball *et al* 2004, Kovalev *et al* 2005, Mehring *et al* 2004, Schulze-Bonhage *et al* 2002). (1) Which decoding accuracy of movement direction can be achieved from multiple channels of ECoG recorded from the human cortex? (2) How is directional information distributed across the lateral convexity of the human cerebral cortex, and which part is suited best for movement direction decoding? (3) Which signal component in time or frequency domain carries most directional information? To address these questions, we recorded ECoG from the dense arrays of platinum electrodes implanted subdurally over fronto-parieto-temporal brain areas in four subjects undergoing evaluation for epilepsy surgery (figure 1, supplementary figures 2–4, available online at stacks.iop.org/JNE/6/016006) while the subjects performed center-out arm reaching movements in four or eight directions, under self-paced and externally cued conditions. Movement-related signals were decoded off-line on a single-trial basis. In both time and frequency domains, we measured the temporally and spatially resolved decoding accuracy (DA) as the probability of correct inference of movement direction. The individual electrode contacts were assigned to the primary motor cortex (M1), premotor cortex (PM), prefrontal cortex (PF) or posterior parietal cortex (PPC) on the basis of anatomical MRI data sets acquired while the electrodes were implanted (Schulze-Bonhage *et al* 2002), and based on the results of direct electrical stimulation of the brain surface through the implanted electrodes. This approach allowed us to accurately map the distribution of directional information in relation to the functional anatomy of the human cerebral cortex.

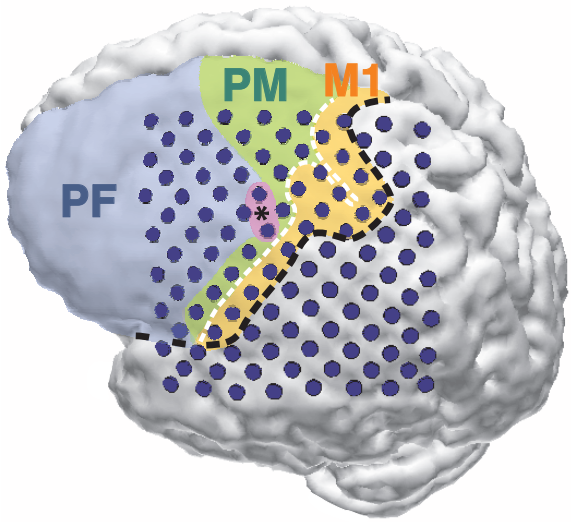

Figure 1. Relation of the subdurally implanted electrode array to the individual brain surface of subject 1, obtained from a whole brain anatomical MRI scan acquired on the day following electrode implantation. The 112-contact platinum electrode grid (4 mm electrode diameter, 7.1 mm inter-electrode distance) covered prefrontal (PF, blue), frontal eye field (∗, purple), premotor (PM, green), primary motor (M1, orange), parietal and temporal areas. White dashed line: precentral sulcus; black dashed line: anatomical border of the frontal cortex (lateral and central sulci).

Materials and methods

Patients

Four patients (aged 55, 42, 20 and 36 years (S1–S4, respectively); S1, S2 and S4 were female) suffering from intractable pharmaco-resistant epilepsy with focal cortical dysplasias in the left fronto-polar resp. right inferior Rolandic cortex were included after having given their informed consent. All patients were strongly right-handed after a modified Oldfield questionnaire (Oldfield 1971) and showed no clinical signs of pareses or other movement disorders. The study was approved by the university clinic's ethics committee.

Experimental methods

All subjects had platinum grid electrodes (4 mm electrode diameter, 112 contacts in subject 1 (cf figure 1) and 3, 64 contacts in subjects 2 and 4, resulting in 7.1 mm and 10 mm inter-electrode distances, respectively) subdurally implanted above fronto-parieto-temporal regions of the left (S1 and S3) and right (S2 and S4) hemisphere, respectively. The site of electrode implantation was exclusively based on the requirements of the clinical evaluation. Two types of experiments were carried out: first, center-out arm movements to four targets, and second, center-out arm movements to eight targets. In all cases, the movement task was carried out with the arm contralateral to the side of electrode implantation (with the right arm in S1 and S3 and with the left arm in S2 and S4). (1) Four-direction experiments: three subjects (S1–S3) performed a self-paced center-out arm reaching task in four directions (right, left, forward, backward) starting from a central position. Both the central starting point and the target points were disks of 4 cm diameter and with a height of 5 mm mounted on an otherwise plane surface. The center-to-center distance from the starting point to the target points was 20 cm. The subjects were instructed to perform natural reaching movements in three dimensions (i.e. not restricted to the horizontal plane), and to touch the target points with the tips of their index and middle fingers. S1 and S3 were instructed to choose the direction of each movement themselves while keeping their eyes closed and to avoid any other movement during the experimental session; S1 participated in two experimental sessions on two separate days and S3 participated in one experimental session. In the experiment with S2 (who participated in one session), movement direction was cued auditorily and the subject had her eyes open as she was unable to perform the purely self-paced task and tended to fall asleep when she had her eyes closed. S2 initiated the reaching movements after a self-chosen interval of at least 2 s after the auditory cue. (2) Eight-direction experiment: one subject (S4) performed one session of an eight-direction task (movements to the same four directions as in the self-paced task and, additionally, also to the four intermediate directions). Because we wanted to ensure similar number of trials for each of the eight movement directions, we chose to visually cue movement direction for this subject. To this end, the subject viewed a LCD display at a 1.5 m distance. At the beginning of a trial, the subject had to press a central button and after a randomly chosen time interval (ranging between 0.75 s and 1.75 s) one out of eight targets (arranged regularly on a circle, 45° apart) was chosen randomly and highlighted visually. The subject then had to move her hand to the target and press the target button.

ECoG from the cortical hemisphere contralateral to the moving arm was recorded using a clinical ac EEG-System (IT-Med, Germany) at 256 Hz (S1, S2, S4) and 512 Hz (S3) sampling rates and 5 s time constant (corresponding to a high-pass filter with 0.032 Hz cutoff frequency). The onset and offset of arm movements were determined based on the digital video (25 Hz sampling rate) synchronized to the ECoG in the self-paced task and on the release of the start button resp. the time when the target button was pressed in the visually cued task. Movement onset and offset was defined based on the first and last visible movement of any part of the upper extremity, including shoulder.

Electrical cortical stimulation

Electrical cortical stimulation through the electrode grid was performed using an INOMED NS 60 stimulator (INOMED, Germany). Trains of 7 s duration consisted of 50 Hz pulses of alternating polarity square waves of 200 μs each. The intensity of stimulation was gradually increased up to 15 mA or to the induction of sensory and/or motor phenomena. All sites with arm or hand motor responses were, in all subjects, located outside the ictal onset zone. The patients were unaware of the timing of stimulation unless motor symptoms occurred.

Anatomical reconstruction

In each subject, a structural MRI data set with full head coverage was acquired after electrode implantation using a T1 MPRAGE sequence. The motor cortices were identified according to anatomical landmarks (Rumeau *et al* 1994, Steinmetz *et al* 1989, Yousry *et al* 1997). The exact relation of the individual electrode contacts to the cortical anatomy was determined using curvilinear reconstructions (Schulze-Bonhage *et al* 2002) and visualized using the CURRY software (NeuroScan, USA). Contacts were classified as primary motor if recording from the precentral gyrus (including electrodes above the central sulcus without motor responses) and if they were either in direct contact to the posterior half of the precentral gyrus or, when located on the anterior half of the precentral gyrus, if they showed motor responses occurring at a low threshold (5 mA). The border between PM and PF was defined based on the location of the frontal eye field (defined as the region with oculomotor responses upon cortical electrical stimulation), the extent of PM as described in the anatomical literature (e.g. Geyer *et al* 2000), and such that PM included all electrode contacts outside M1 with motor responses. Electrodes with oculomotor responses or upper extremity sensory responses were excluded from the M1, PM and PF electrode groups, and also from the group of frontal cortex electrodes (FC), which was defined as the combination of M1, PM and PF electrodes. A representative result of this procedure is shown in figure 1 for subject S1. In S1 and S3, the seizure onset zone was located outside the electrode grid

(left fronto-polar cortex in S1, both left orbito-fronto-polar and left lateral temporal cortex in S3). In S2 and S4, the seizure onset zone was located within the grid, but was distinct from the area with hand and arm movement responses in both cases (seizure onset zones were in right primary sensori-motor face area in S3 and right lateral prefrontal cortex in S4).

Time–frequency analysis

The time-resolved amplitude spectra of all recording channels were calculated for each trial individually by multi-tapering spectral analysis methods using a time window of 500 ms duration and three Slepian tapers (Percival and Walden 2002). The time step was 1/32 s. To dissect amplitude changes for different frequencies during the time course of the trial, we computed relative power spectra in the following way (cf Rickert *et al* 2005). For each frequency bin, we divided the time-resolved amplitude by the baseline amplitude for this frequency. The latter was determined as the mean power of the frequency in the time interval between 1500 and 1000 ms before the onset of the movement, averaged across trials (i.e. all trials of the corresponding channel).

Inference of movement direction

To assess the topography of directional information, we analyzed the following complementary aspects: first, we decoded from local electrode groups within a narrow spatial sliding window covering a square area of approximately 1 cm^2. Maps obtained in this way enabled us to visualize the detailed spatial distribution of local decoding accuracy throughout the grid. The decoding accuracy obtainable from simultaneously decoding from the whole group of channels assigned to the individual frontal cortical subdivisions (M1, PM, PF) can, however, not be derived from the local DA maps, which are based on simultaneously decoding from a small, local group of recording channels, because long-range (i.e. beyond the scale of the local group of channels) correlations are not captured. Therefore, we also computed the DA based on the whole set of electrodes in M1, PM and PF. Additionally, we determined the dependence of extractable information on the number of channels used for decoding. This may be of considerable practical relevance, especially in the likely case that the number of recording channels for chronic implantation in human patients should be kept as small as possible.

We decoded the ECoG signals on a single-trial basis by regularized linear discriminant analysis (RLDA, Friedman 1989). Using the RLDA, we analyzed either the smoothed ECoG signals (filtered by a Savitzky–Golay filter of second order and 181 or 361 sampling points width for 256 Hz and 512 Hz sampling frequency, respectively) or the amplitude modulations of different frequency bands. For both cases, signals from two different time windows were used separately: (i) peri-movement time window: signals between 250 ms before movement onset and movement end were used; (ii) pre-movement time window: signals up to 250 ms prior to movement onset were used.

To quantify the decoding accuracy (DA), we calculated the percentage of trials which could be correctly classified.

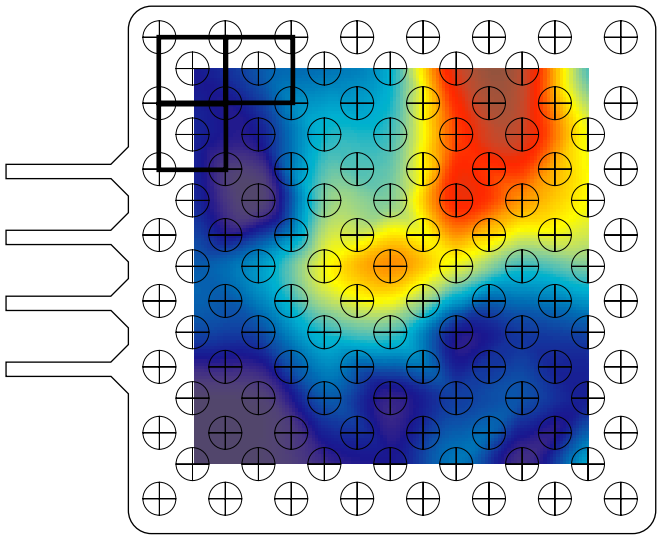

Figure 2. Definition of local decoding accuracy (DA). Local DA map (as in figure 3) shown in relation to the implanted electrode array with 112 electrodes. Local DA was determined using electrodes in a 1 cm × 1 cm sliding window (black boxes), which was moved in 1 cm steps through the whole grid. All windows, except the one in the top right corner, contained five electrodes. The DA of a local group was always assigned to the center of the window, resulting in a map of 7 × 7 values, which was displayed using bicubic interpolation. For the 8 × 8 contact grid, used in subject 2, each window contained only four electrodes, as in this case there were no central electrodes.

To this end, we performed ten times ten-fold cross-validation (Efron and Tibshirani 1998); thus, trials used to train the discriminant were not included in the test set for decoding. For each training set, an individual regularization parameter of the RLDA (Friedman 1989) was computed by optimization across the training data. To establish a significant DA, the mean DA was tested against a binomial distribution (see Mehring *et al* (2003)).

Local DA was determined by decoding from groups of electrodes covering 1 cm × 1 cm of the grid (see figure 2). To test whether two distributions of local DA exhibited a significantly different median, we used the Wilcoxon rank sum test for equality of medians. The time-resolved DA was computed by decoding the activity in a sliding window of 500 ms duration. The window was shifted in time steps of 50 ms from −1.5 s to +1.5 s around movement onset. Electrodes with oculomotor responses or upper extremity sensory responses were excluded from all analyses, except for mapping of local DA.

Tuning analysis

Tuning curves were obtained by computing the trial-averaged signal values separately for each target direction. To establish significant tuning, we computed the signal-to-noise ratio (SNR) of the tuning curve by the following equation:

$$\mathrm{SNR} = \frac{\sigma_s^2 - \sigma_b^2}{\sigma_n^2}.$$

Here, σ_s^2 is the variance of the tuning curve, σ_n^2 is the variance of the trial-by-trial fluctuations and σ_b^2 is the variance of the

tuning curve that is induced in the presence of noise if only a limited number of trials are measured for each direction. Under the assumption of a Gaussian noise distribution, an estimate for this term is

$$\sigma_b^2 = \frac{1}{8N}\sum_{\mathrm{tr}=1}^{8}\sigma_{\mathrm{tr}}^2$$

where σ_{tr}^2 are the variances of the trial-by-trial fluctuations for each specific target tr, and N is the number of trials for each target. To compute the significance level (p-value) of the tuning, we compared the SNR value to the chance distribution for a flat tuning curve. The chance distribution was obtained numerically by computing 1000 times the SNR of the same signals with a random relation between signals and directions. For significantly ($p < 0.05$, see above) tuned signals, we investigated whether the directional modulation was cosine-like. To this end, we fitted a cosine function ($y = a + b\cos(x) + c\sin(x) = a + d\cos(x - \varphi)$, with φ being the preferred direction) to the trial-averaged signal by a least-squares fit.

To compare tuning curves of different signal components (e.g. movement-related potentials (MRPs), spectral amplitude modulations in different frequency bands) and of different channels, normalized tuning curves were calculated according to the following procedure: (i) the mean of the tuning curve (i.e. the mean across all directions) was subtracted; (ii) the resulting values were divided by the standard deviation of the trial-by-trial fluctuations (i.e. the fluctuations around the mean signal value of each target). The experimental data of subject 1 included two recording sessions from two different days. All results were reproducible for the two recording sessions of subject 1 and we therefore averaged for this subject all results across these two sessions, except for the results for parietal electrodes which are reported for both recording days, separately.

Results

In this section, we first present all results for the four-direction center-out experiments before the results from the eight-direction experiments are described in an additional paragraph at the end of the section.

Time–frequency responses and directional modulation in different ECoG frequency bands

Distinct mean time–frequency responses were obtained for the primary motor, premotor and prefrontal cortex (figure 3(a)–(c)). In M1, very pronounced effects were as follows: a sustained decrease in relative spectral power most prominent from approximately 6 to 30 Hz, starting approximately 500 ms before movement onset, and a sustained increase in spectral power in the range of 50 Hz to above 100 Hz, starting approximately 200 ms before movement onset. In contrast, the band from approximately 30 to 50 Hz showed less movement-related power modulation. Movement-related responses were attenuated in the premotor cortex and nearly absent in the prefrontal cortex. Based on the grand mean amplitude spectra of M1 and PM electrodes, we delineated five frequency bands for further analysis: a low frequency (<2 Hz) band, an intermediate (6–30 Hz) frequency band including the alpha and beta range, and a low gamma band (34–48 Hz), a high gamma band (52–128 Hz) and a 'broad' gamma band (34–128 Hz). Movement-related power decreases were typically found in the alpha/beta and in the low gamma band; power increases in the high gamma band (figure 3), while the low frequency band showed both power increases and decreases (figure 3(d), first panel). Note that the low frequency band of the time–frequency responses is different from the smoothed ECoG insofar as the former reflects power changes irrespective of the phase of the signal relative to movement onset, while in the latter the phase information is conserved. In the next paragraph, results derived from power in the low and other frequency bands are described. Results based on the smoothed ECoG—referred to as movement-related potentials (MRPs)—are then described in the following section.

To determine whether modulations with respect to movement direction were similar or different in the five frequency bands, we determined, for each motor cortical channel from each subject, the movement direction with the maximal and with the minimal response in the low frequency band (figure 3(d), left panel). Then, for these two selected movement directions, we computed the average responses in the other frequency bands (figure 3(d), second to the fifth panel). For these other frequency bands, we observed only very little response differences. The same analysis was then repeated for the movement directions which maximized the response difference in the intermediate frequency band (figure 3(e)). If these directions in the latter case were the same as in the first case, the overall picture would remain essentially the same. Interestingly, this was not what we observed; instead, when maximizing the response differences for the intermediate frequency band, considerably smaller response differences than before resulted in the low frequency band (figure 3(d) left panel compared to figure 3(e) left panel), indicating that the directions with maximal response differences in the low and intermediate frequency band were not identical. Also the gamma band amplitude modulations were maximal resp. minimal for other movement directions than spectral amplitude modulations in the intermediate and low frequency band, respectively (figure 3(f)). The high gamma (52–128 Hz) and the 'broad' gamma band (34–128 Hz) showed maximal resp. minimal activities for similar movement directions (figure 3(g), (h)). Taken together, these results corroborated our decision to treat these different frequency bands separately for the further examinations.

Spatially resolved direction decoding

To address the spatial distribution of DA within the frontal cortex, we decoded from local electrode groups covering a square of approximately 1 cm^2 area (see the Materials and methods section for further details), using either the MRP (for examples of the MRPs, see supplementary figure 1, available online at stacks.iop.org/JNE/6/016006) or the time course of spectral power changes in the five frequency

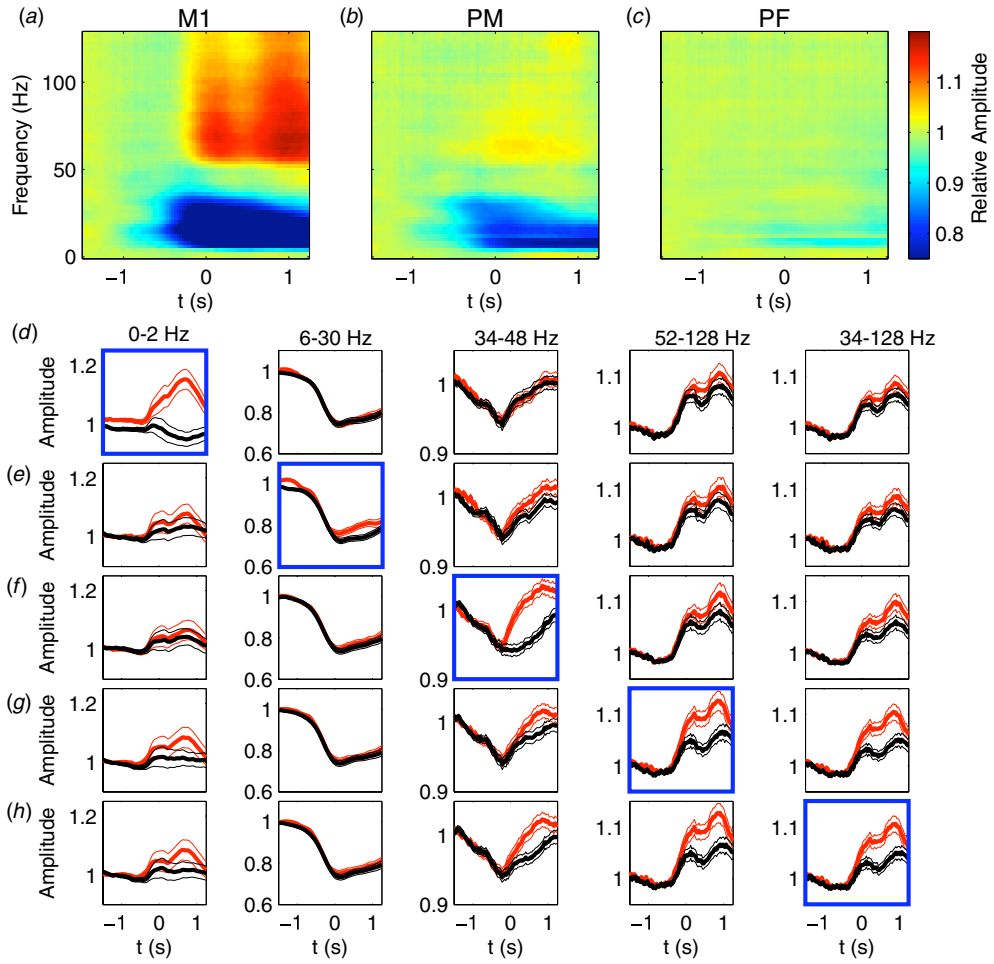

Figure 3. Mean spectral power changes in the frontal cortex and directional modulation of ECoG frequency bands (four movement directions). (a)–(c) Mean relative time-resolved spectral power changes across all four subjects, for all channels recording from the primary motor cortex (a), from the premotor cortex (b) and from the prefrontal cortex (c). Time is indicated relative to movement onset. (d) For each channel, the two movement directions with the maximal and minimal response (i.e. maximal and minimal relative spectral power change) in the low frequency band (<2 Hz, indicated by a blue box) were selected. The black and red curves show the mean time course of spectral power changes, and its standard error of the mean, across all motor cortical channels from all subjects for the minimal (black) and maximal (red) response. In the remaining four panels, mean responses for the same selection of movement directions as in the left panel (here: maximizing directional modulation in the low frequency band) are shown for the other frequency bands investigated, i.e. 6–30 Hz, 34–48 Hz (low gamma band), 52–128 Hz (high gamma band) and 34–128 Hz ('broad' gamma band). In (e), the same analysis was carried out, but now the response differences were maximized for the intermediate frequency band (marked by a blue box), while again the same data selection was used in the remaining panels (i.e. for the other frequency bands). In (f), movement directions were selected to maximize directional differences in the low gamma band (corresponding to the third panel), in (g) for the high gamma band, and in (f) for the 'broad' gamma band.

bands as described above. An example of the spatial DA distribution in relation to both anatomical landmarks and cortical responses upon electrical stimulation is shown in figure 4. The corresponding results for the other subjects are provided in the supplementary material available online at stacks.iop.org/JNE/6/016006. The maxima of local DA were typically found in the same area where electrical stimulation elicited hand or arm motor responses, i.e. in the superior part of the precentral gyrus. This pattern was most consistently observed for the decoding of the MRPs, for low frequency spectral decoding and for gamma band spectral decoding. Across subjects, average local DA of MRPs was highest in M1 (median: 50%), intermediate in PM (median: 40%) and lowest in PF (median: 29%). The difference between M1/PM and PF was statistically significant ($p < 0.001$, Wilcoxon rank sum test for equality of medians).

To further quantify the contributions of the various frontal cortical subregions, we performed movement direction inference for the entire sets of channels recording from each of the three frontal cortex subdivisions (M1, PM and PF) individually and for different combinations: from the 'motor cortex' (MC = M1 + PM) and from the combination of the premotor and prefrontal cortex (PM + PF). Importantly, for these and all further analyses, no spatial sliding window was used to prevent the mixing of signals from neighboring anatomical areas. For MC, this analysis was also carried out separately for each of the three different frequency bands (low, intermediate and gamma band). Moreover, all comparisons were computed separately for two different time windows (pre-

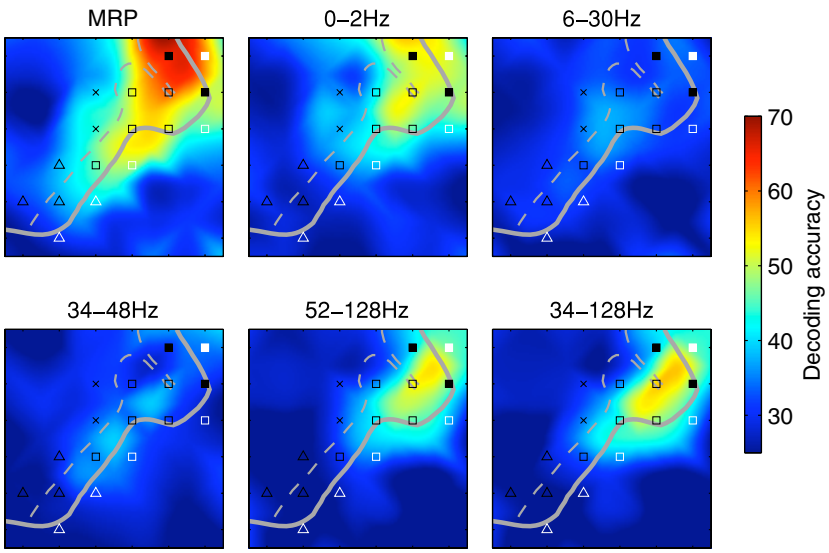

Figure 4. Spatially resolved decoding accuracy (DA) for movement-related potentials (MRPs) and amplitude modulations in different frequency bands. Color-coded DA maps of subject 1 performing a four-direction center-out task derived from local electrode quintets (see the Materials and methods section for further details). Note the close spatial correspondence of sites with high local DA and sites with arm resp. hand motor responses upon direct electrical cortical stimulation (filled and empty black squares), both located in the superior part of the precentral gyrus. Crosses: oculomotor responses; white squares: arm and hand sensory responses; black and white triangles: motor and sensory orofacial responses. The same cortical sulci as in figure 1(a) are displayed as gray dashed lines.

movement time window, and mean movement duration time window). The results are summarized in figure 5. We found that MC (average DA across subjects: 76%/45% for peri-movement and pre-movement activity) and M1 (71%/43%) consistently yielded higher DA than PM (53%/31%), and PM yielded higher DA than PF (38%/24%), but PF still yielded significant DA ($p < 0.01$, see the Materials and methods section) in two out of four subjects. There was no significant difference ($p > 0.1$, Wilcoxon signed rank test) in DA based on PM alone as compared to PM + PF (54%/25%). Furthermore, both the low frequency and the high gamma bands showed higher DA than the intermediate frequency band (average DA across sessions: 62%/35%, 39%/28%, 36%/27%, 53%/31%, 54%/31% for the low, intermediate and gamma bands for peri-/pre-movement activity). These results were consistently found in both time windows investigated, although with overall lower DA for the pre-movement time window.

In three of the subjects investigated, there were ECoG channels above the posterior parietal cortex. For these subjects, the decoding accuracies of the posterior parietal cortex for MRPs in the peri-movement time window were 50%, 23% (P1 sessions 1 and 2), 54% (P3) and 39% (P4).

Because the numbers of electrodes varied considerably between M1, PM and PF both within and across subjects, we calculated the dependence of DA on the number of electrodes for the full range from one single electrode to the total numbers of electrode recordings from each area in each subject. Similar to the random neuron dropping curves by Wessberg *et al* (2000) and the analyses by Shenoy *et al* (2003), we computed curves based on the average DA obtained from 50 randomly drawn sets of electrodes for each set size, separately for all four signal components studied (MRP and low, intermediate and gamma bands). The results are shown in figure 6. For M1, electrode dropping (ED) curves (red) rose monotonically with the number of electrodes and were continuously above the ED curves of PF (blue). This was observed for all four signal components investigated. For PM (green), time domain decoding, low frequency spectral decoding and gamma decoding resulted in ED curves between those for M1 and PF. The generally lowest gradient was observed in the ED curves of the prefrontal cortex (PF, blue).

Direction decoding from all possible frequency bands

Results on directional information from all possible frequency bands are summarized in figure 7, showing the decoding accuracy for the peri-movement time window of all motor cortex channels averaged across all experimental sessions. For decoding from all possible frequency bands, we used all possible combinations of lower and upper frequency bounds (from 0.032 Hz to 128 Hz, 2 Hz resolution). These results show that narrow frequency bands of <10 Hz width generally yield low decoding accuracy with only one exception: the only narrow frequency bands with high DA were those bands including the very low frequencies, corresponding to the upper-left corner in figure 7. Besides the high DA of this narrow, low frequency band, high DA was also reached if (1) the lower frequency bound of the analyzed frequency band was below approximately 60 Hz and (2) the higher frequency bound was higher than approximately 100 Hz. Frequency bands meeting both of these criteria correspond to the upper-right field of the plot in figure 7. In contrast, all possible frequency bands within the 6–30 Hz range yielded low DA. None of these latter frequency bands had significantly higher DA than the whole 6–30 Hz band ($p > 0.8$, Wilcoxon sign

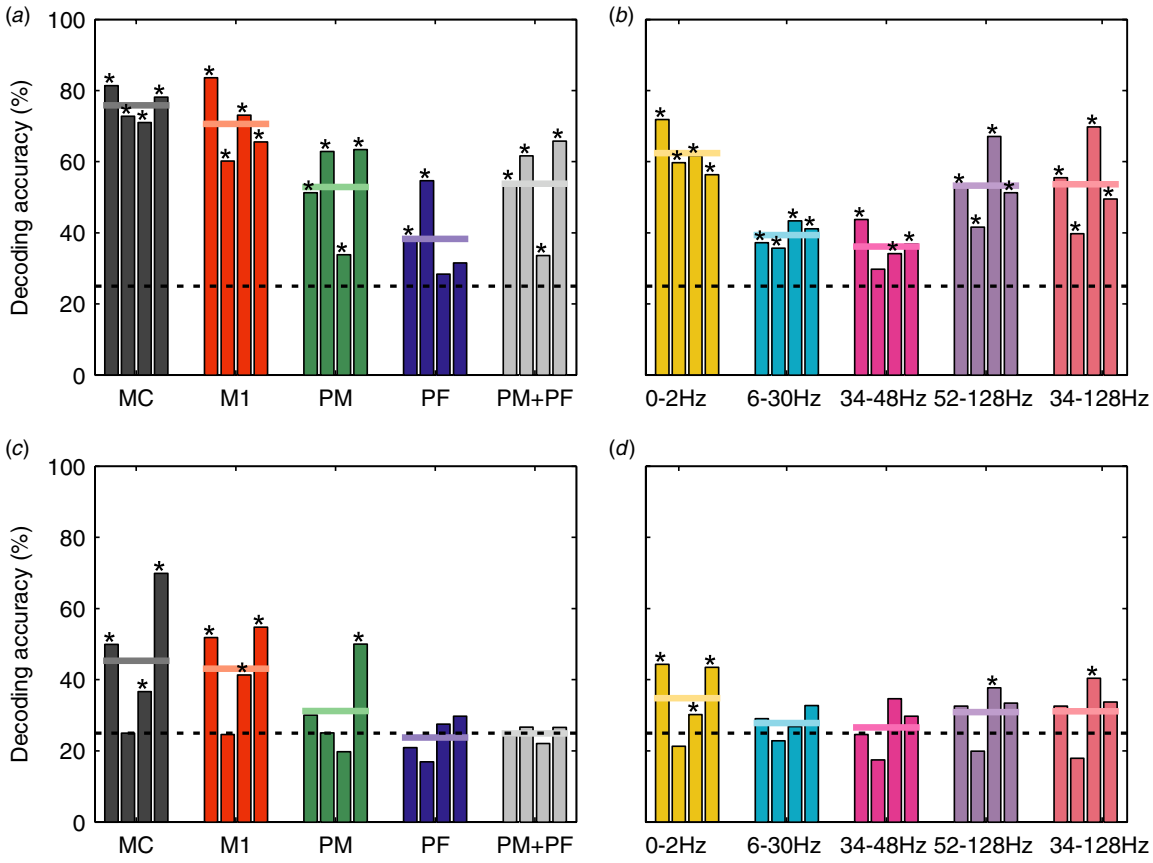

Figure 5. Decoding accuracy from different frontal anatomical subregions and signal frequency bands (four movement directions). The dashed line depicts the chance level. Stars indicate bars with significant decoding accuracy ($p < 0.01$, see the Materials and methods section). (a) Decoding results for the movement-related potentials from the whole mean duration of the reaching movement, including activity up to 250 ms prior to movement onset ('peri-movement time window'). The five groups of bars correspond to the anatomical subdivisions MC (entire motor cortex = M1 + PM), M1 (primary motor cortex), PM (premotor cortex), PF (prefrontal cortex) and PM + PF (premotor and prefrontal cortex). Each of the five bars in the individual groups of bars represents one recording session (two sessions from subject 1, and one session from each of the subjects 2, 3 and 4). Horizontal colored lines mark the mean DA for each anatomical subdivision; the black dashed line marks the chance level. (b) Frequency domain decoding results for MC, for the same time window as in (a), for the low, intermediate and different gamma bands (low, high and broad). All conventions and the scaling of the *y*-axis are as in (a). In (c) and (d), the corresponding results as in (a) and (b) are given for activity during the pre-movement time window only, ranging from 250 ms to 0 ms before arm movement onset.

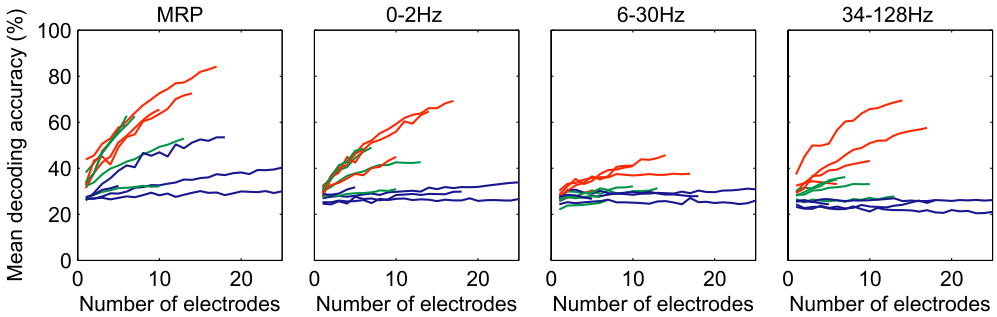

Figure 6. Decoding accuracy as a function of the number of electrodes. Similar to the random neuron dropping curves by Wessberg *et al* (2000) and the analyses by Shenoy *et al* (2003), the average DA obtained from 50 randomly drawn sets of electrodes is plotted as a function of the number of electrodes in each set. Each curve represents one of the three frontal cortical subdivisions of one of the subjects. The different lengths of the curves are due to the different total number of channels recording from the three subdivisions in the individual subjects. Red: M1; green: PM; blue: PF.

rank test). Thus, the beta band from 18 to 22 Hz yielded a lower decoding accuracy (average across subjects: 32%, for motor cortex channels and the peri-movement time window) than the 'intermediate' frequency band (6–30 Hz, average across subjects: 39%). Therefore, the low decoding accuracy obtained from the 'intermediate' frequency band was not

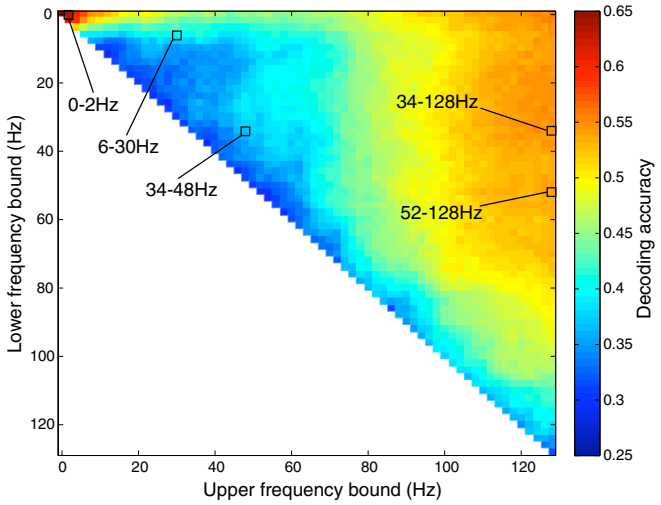

Figure 7. Results on directional information from all possible frequency bands. Color-coded decoding accuracy (DA) for the peri-movement time window of all motor cortex channels averaged across all experimental sessions is shown. For movement direction inference, all possible combinations of lower and upper frequency bound of the analyzed frequency band (from 0.032 Hz to 128 Hz, 2 Hz resolution) were used, as indicated for the *x*- and *y*-axes. Additionally, the DA values for the five frequency bands systematically investigated in our study are indicated.

related to its (relatively large) width, i.e. the fact that it included both alpha and beta frequencies.

Temporally resolved direction decoding

The results presented in the previous section indicate that activity before actual movement onset already contained considerable directional information. To further quantify the temporal evolution of DA, we computed the time course of DA relative to movement onset using a sliding window (figure 8(a); window length: 500 ms). Time courses based on either M1 (red) or MC (black) showed a steep rise in DA already approximately 200 ms before movement onset. The same holds for PM (green), albeit with a somewhat less steep rise. By contrast, prefrontal DA (blue) rose more slowly and only after movement onset. A broad peak in decoding accuracy was reached at about 500 ms after movement onset for M1 and MC, and at approximately 1000 ms after movement onset for PM and PF. For decoding accuracy from spectral amplitude modulations (figure 8(b)), the most pronounced increases in DA were observed for decoding from primary motor MRPs, from the primary motor high gamma band and from the primary motor broad gamma band. The time course for these bands was very similar to the time course of MRP based decoding from M1 and MC (red and black curves in figure 8(a)).

Eight-direction decoding and cosine directional tuning

Finally, we investigated how our findings on decoding of four discrete movement directions extend to the case of eight

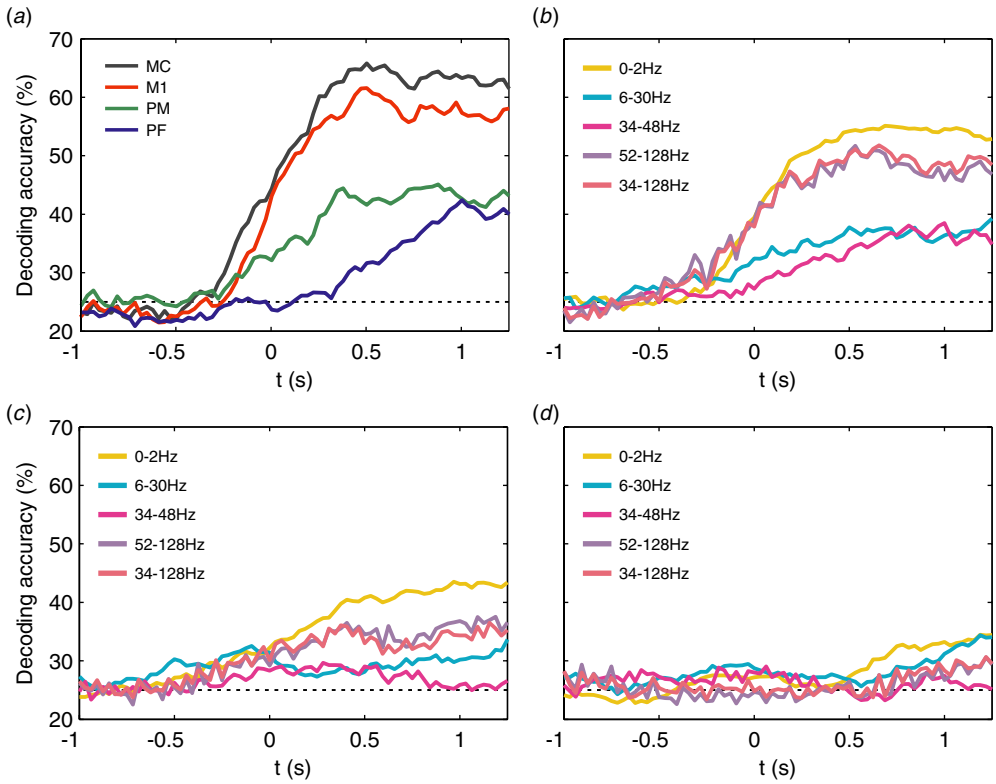

Figure 8. Temporal evolution of decoding accuracy (four movement directions). Graphs show the DA of the time window lasting from 500 ms before until the time indicated on the *x*-axis. Time is given relative to movement onset. (a) Time course for decoding of the movement-related potentials for M1, PM, MC and PF. (b) Time course of DA for decoding from the amplitude spectra using the low, intermediate and different gamma bands for M1. The black line indicates the chance level. (c) Time course for PM and (d) for PF.

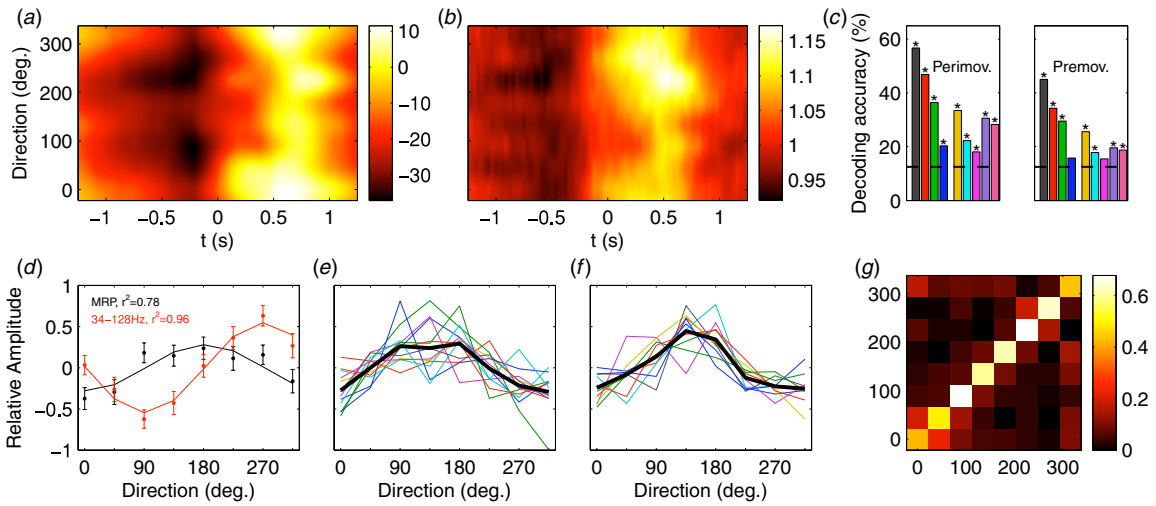

Figure 9. Neuronal tuning and decoding of eight movement directions. (a) and (b) Time-resolved tuning of one individual channel (recorded from the primary motor cortex of subject S4) as an example for the dependence of movement-related potentials (a; in μV) and gamma band relative spectral power changes (b; based on the 'broad' gamma band, given in %) on the movement angle. Time axis is relative to movement onset. (c) Decoding results for the frontal anatomical subdivisions and for the five investigated frequency bands. Color conventions as in figure 5. Left panel: entire movement time window (corresponding to figures 5(a), (b)); right panel: pre-movement time window (corresponding to figures 5(c), (d)). The dashed line depicts the chance level. Stars indicate bars with significant decoding accuracy ($p < 0.01$, see the Materials and methods section). (d) Normalized tuning curves (cf the Materials and methods section) and cosine fit of MRP (black) and 'broad' gamma band activity (red) of the channel depicted in (a) and (b). Black and red dots: mean measured MRP and relative gamma spectral amplitude for each movement angle, respectively. Error bars denote standard error of the mean. (e) and (f) Single channel normalized tuning curves (cf the Materials and methods section) for all motor cortical channels, aligned according to each channel's preferred direction. Black line: mean across all channels. (e) MRP; (f) 'broad' gamma band activity; (g) confusion matrix for MRP-based eight-direction decoding; *x*-axis: decoded movement direction; *y*-axis: true movement direction. The probability that the decoding algorithm predicted each of the eight possible directions, given the true direction, is color coded, showing that each movement direction could be discerned from all other directions with reasonable accuracy, and that error assignments occurred mostly to nearest-neighbor directions.

directions. Examples for the dependence of MRPs and gamma band spectral power changes on movement direction for a primary motor electrode are shown in figures 9(a) and (b). Qualitatively, these examples suggest that the concept of a unimodal directional tuning might hold true for these signals, since they show a quite steady slope from high activity when moving in a 'preferred' direction to lower activity when moving in an 'anti-preferred' direction. Decoding results for the data of eight movement directions are shown in figure 9(c). Although overall DA was lower than that for the four directions, DA still approached 60% correctly inferred trials when decoding from motor cortical MRPs (MC, black). The typical DA differences seen earlier for the four-direction decoding results between M1, PM and PF (figure 5(a)) were also observed for the eight direction results (figure 9(c)). The same was true for the DA differences between the five frequency bands investigated (figure 9(c) compared to figure 5(b)). The confusion matrix based on MRP decoding shown in figure 9(g) demonstrates that each of the eight movement directions could be discerned from all other directions with reasonable accuracy, and that error assignments were mostly confined to immediately neighboring directions.

Results from a quantitative analysis of ECoG tuning curve shape are displayed in figures 9(d)–(f). A cosine function was fitted to all significantly tuned channels ($p < 0.05$) and the correlation between the fit and the trial-averaged signal was computed (see the Materials and methods section for further details). The squared correlation coefficient was 0.60 for MRPs and 0.67 for gamma band (34–128 Hz) activity, respectively, indicating that ECoG tuning can be well described by cosine tuning.

Discussion

In the present study, we confirmed the feasibility of accurate inference of the direction of center-out arm reaching movements from movement-related epicortical field potentials, and from their spectral amplitude modulations, recorded directly from the surface of the human frontal and parietal lobe. We found DA in the same range as had been previously obtained from multiple micro-electrode, single-neuron and local field potential recordings from the monkey primary motor cortex during an eight-direction task (Mehring *et al* 2003). In contrast to the relatively low decoding accuracy values we had previously obtained from single channels of motor cortical ECoG (Mehring *et al* 2004), decoding multiple ECoG channels simultaneously resulted in substantially higher DA, rendering them more suitable for practical applications.

The present study is, to our knowledge, the first quantitative topographic analysis of directional information on goal directed arm movements in the human cerebral cortex based on exact assignments of recording sites to the individual cortical anatomy and on results from functional electrical stimulation through the electrodes. Previous studies were either restricted to small stretches of cortex

(Mehring *et al* 2004, Rizzuto *et al* 2005) or lacking similarly precise anatomical and functional localization of the electrode contacts used for decoding (Leuthardt *et al* 2004, 2006, Schalk *et al* 2007). In Leuthardt *et al* (2004), electrical stimulation mapping was performed, but the topographical correlations between electrical stimulation and movement or imagery were reported as not strong enough to support clear conclusions. Knowledge about the spatial distribution of directional information and of the best signal components for movement inference is essential for the development of BMIs based on cortical surface recordings for a potential clinical application. We examined recordings from dense arrays of electrodes covering approximately 7 cm × 7 cm of the exposed brain surface and localized the individual electrodes in whole head MRI scans obtained while the electrodes were implanted. In conjunction with direct cortical electrical stimulation through the implanted electrodes, this allowed us to assign each recording channel exactly to the structural and functional cortical anatomy.

The results of our study indicated that, among the different frontal and parietal regions investigated, the region of cortex on the exposed surface of the precentral gyrus showing hand/arm responses upon electrical stimulation yielded the highest direction-related signal modulation. This prominent position of the precentral gyrus was equally observed under self-paced and externally cued conditions, and for decoding from the movement-related potentials in the time domain and from the gamma frequency range. The overall highest decoding accuracy was obtained from slow movement-related potentials (MRPs). In the case of self-paced voluntary movements, MRPs can be subdivided into the readiness potential and the motor potential occurring before and during movement execution, respectively (Ball *et al* 1999, Kornhuber and Deecke 1965, Shibasaki and Hallett 2006). Because decoding accuracy peaked during movement execution, it follows that mainly the motor potential was responsible for the high decoding accuracy obtained from the motor cortex.

A predominance of information about the parameters of two-dimensional joystick movements in the ECoG recorded from primary and premotor areas was recently reported, but the relative contribution of M1 and PM varied for different signal components and kinematic parameters (Schalk *et al* 2007). In contrast, we have consistently found the highest amount of directional information in the hand and arm representation area of the precentral gyrus. This different result may be due to the fact that in our study anatomical assignments were based on the cortical anatomy from patients' individual structural MR scans while Schalk *et al* used a brain template, but might possibly also be related to the different experimental movement paradigms. The strong visuomotor component of the task in the study of Schalk *et al* where subjects controlled a cursor on a video screen to track a target in two dimensions may have resulted in a greater involvement of the premotor areas as compared to the tasks used in our study (cf Schwartz *et al* 2004).

In BMI-related animal research, to our knowledge, the closest counterpart to our experiments is the work of Hatsopoulos *et al* who decoded discrete and continuous arm movement targets from the motor cortex of rhesus monkeys (Hatsopoulos *et al* 2004). While Hatsopoulos and colleagues found that continuous decoding was most accurate when based on single cell activity of M1 neurons, activity from an area designated as dorsal PM (PMd) predicted discrete movement direction more precisely than an equally sized M1 ensemble. Possible reasons for this discrepancy include more subtle task differences or performance differences, differences due to the use of neuronal spiking activity versus ECoG, true species differences in the organization of the motor cortex, or also the general difficulty in delineating the functional border between M1 and PM (see Stepniewska *et al* (1993)).

In addition to the high DA obtained from the precentral gyrus, we found gradually less, but still significant directional information in PM and PF. This was consistently observed in the different aspects of topographic analysis (see above) as well as for the different signal components. Spatial selectivity during arm movements in the prefrontal cortex may seem surprising, but was recently also described for EEG recorded using intracerebral depth electrodes (Rizzuto *et al* 2005). The gradient of directional information from M1 over PM to the dorsolateral PF supports the view of a functional gradient of motor functions in the human frontal cortex, with M1 most closely related to encoding of kinematic movement parameters. PM neurons encode the relative position of reaching target, hand and eye (Pesaran *et al* 2006). PM and PF are preferentially involved in higher order motor functions and more cognitive aspects of motor control (Ball *et al* 1999, Fuster 2000, Geyer *et al* 2000). For some subjects, the decoding accuracy of PM + PF was lower than the decoding accuracy of PM alone. This has the following reason: for decoding PM + PF signals, far more electrodes are used than for decoding PM. Thus, the dimension of the decoded feature vector is higher and the decoder needs to estimate more parameters from the training data. If the additional signals contain no or only a very small amount of directional information, the decoding accuracy can, therefore, decrease due to overfitting of the decoder on the training data. An interesting perspective in respect of its topographic distribution would be to investigate whether movement-related information predominates in certain parts of the prefrontal cortex, possibly those close to the border to PM.

With respect to clinical BMI application, our results suggest that epicortical recordings from premotor and prefrontal regions may be used in cases where informative M1 signals are lost due to pathological alterations. However, also the posterior parietal cortex (PPC) holds promise as a source of control signals for BMIs (Andersen *et al* 2004, Pesaran *et al* 2002, Scherberger and Andersen 2007). Of the PPC subregions, the parietal reach region (PRR) has in particular received attention because activity in PRR indicates the goal of a reach in visual coordinates (Batista *et al* 1999). Scherberger and colleagues found that LFP signals in PRR predict the direction of currently planned reach and eye movement from single-trial information (Scherberger and Andersen 2007). In humans, a likely homologue to the monkey PRR was identified using functional MRI (fMRI) and found to be located in the superior parietal lobule, close to the mesial part of the

parietal lobe (Connolly *et al* 2003, Fernandez-Ruiz *et al* 2007, Medendorp *et al* 2003). In our study, two patients performed the motor task with their eyes closed, ruling out visual information as an explanation for movement-related response differences (P1 and P3). Significant directional information was found in parietal signals in both P1 and P3. The part of the PPC that was covered by the electrode grids consisted, in both cases, mostly of the anterior-most part of the inferior parietal lobule (figure 1 and supplementary figure 3, available online at stacks.iop.org/JNE/6/016006). Therefore, it is unlikely that the parietal signals in our study originated in the PRR which would be assumed much more medial. Comparing recordings from the human PRR region would be an interesting issue for future investigations, as this area might provide better movement discriminability than the inferior parietal cortex and also plays an important role in free choices of motor behavior (Pesaran *et al* 2008).

Examining the ECoG in the frequency domain, we consistently found two pronounced effects in motor cortex channels. (1) A sustained decrease in spectral power most prominent from approximately 6 to 30 Hz and starting approximately 500 ms before movement onset, corresponding to the so-called movement-related 'desynchronization' (Crone *et al* 1998b, Pfurtscheller and Lopes da Silva 1999). This power decrease involved the alpha, beta and the low gamma band (figure 3). LFP recordings from the monkey motor cortex indicate that in particular the depression of beta activity is specific for movement execution in contrast to movement observation, which resulted in increased beta band activity (Tkach *et al* 2007). (2) A sustained increase in spectral power in the high gamma band, from approximately 50 Hz to above 100 Hz and starting approximately 200 ms before movement onset, similar to many previous studies in epilepsy patients (Aoki *et al* 1999, Arroyo *et al* 1993, Ball *et al* 2004, Brovelli *et al* 2005, Crone *et al* 1998a, Pfurtscheller *et al* 2003, Sinai *et al* 2005, Tanji *et al* 2005). This high gamma band activity has been described to closely correlate to cortical electrical stimulation mapping (Crone *et al* 1998a, Miller *et al* 2007). In the present study, we showed that during center-out arm movements high gamma power is very pronounced in the mean response of channels recorded from the precentral gyrus, but not in the mean response of premotor and prefrontal channels. Recently we succeeded in recording high gamma band activity above the Rolandic cortex at similarly high frequencies as in the present study using EEG recorded from the scalp surface of healthy subjects (Ball *et al* 2008). Together with recent MEG findings (Cheyne *et al* 2008, Dalal *et al* 2007, 2008, Tecchio *et al* 2008, Waldert *et al* 2008), this indicates that high gamma band movement-related oscillations in human subjects are not a pathologic phenomenon only observed in epilepsy patients.

Considering the different reactivity of different frequency bands with respect to voluntary movement as discussed in the preceding paragraph, identifying the optimal frequency band(s) for spectral-power-based decoding is an important issue that has been extensively addressed in the BMI context (Leuthardt *et al* 2006, Miller *et al* 2008, Rickert *et al* 2005, Schalk *et al* 2007, 2008, Shenoy *et al* 2008, Stark and Abeles 2007, Wilson *et al* 2006, Wisneski *et al* 2008). Based on the time course of grand mean amplitude spectral changes of M1 and PM electrodes, we delineated five frequency bands for further analysis: a low frequency (<2 Hz) band, an intermediate (6–30 Hz) frequency band including the alpha and beta range, a low gamma band (34–48 Hz) and a high gamma band (52–128 Hz) (figure 3). Furthermore, we also analyzed a broad gamma band including both the low and high gamma band (34–128 Hz). We found high decoding accuracy of arm movement direction based on amplitude modulation both in the low frequency band (<2 Hz) and in the high gamma band (52–128 Hz). Both of these bands yielded considerably higher decoding accuracy than the alpha, beta and low gamma bands. Although the power depression in the alpha and beta bands precedes the power increase in the high gamma band (Crone *et al* 1998a, 1998b, cf also figure 3), no similarly pronounced differences in the timing of DA based on these frequency bands were observed. In summary, our findings show that the low gamma band typically shows a movement-related power decrease as do the alpha and beta bands. Furthermore, with respect to arm movement direction during a center-out task, the low gamma band shares a relatively low DA with both the alpha and beta bands. Therefore, the low gamma band may be functionally more similar to the alpha and beta bands than to the high gamma band (see also Crone *et al* 1998a 1998b, Miller *et al* 2007, Rickert *et al* 2005).

In Miller *et al* (2008), decoding accuracy was evaluated for hand versus rest, tongue versus rest and tongue versus hand classifications, while in our study the classes to be separated were arm movements to different directions. Together with the slightly different boundaries of the frequency bands investigated, this may be an explanation for differences in the results of the study of Miller *et al* (2008) and our study (e.g. the better DA of low than of high gamma activity for hand versus rest classification, that is in contrast with our results). The high frequency band from 76 to 150 Hz yielding the best decoding accuracy in the study of Miller *et al* could not be systematically investigated in our study because of too low sampling frequency. Therefore, the information content of very high frequency ECoG activity with respect to movement parameters might be underestimated in our study.

A difference between amplitude modulation in the low frequency band (<2 Hz) and the smoothed ECoG is that the former only contains power amplitude information while the latter also contains information about signal phase relative to movement onset. The finding that also the low frequency component contained directional information indicates that not all of the directional information that is found in the smoothed ECoG can be attributed to directional differences in the signal phase.

DA from monkey motor cortical LFP spectra was examined by Rickert *et al* (2005), likewise during a center-out task and using regularized linear discriminant analysis for decoding as applied in the present study. The general picture in that and in the present study is remarkably similar. An intermediate 'gap' with little or no significant directional information extended from 13 to 63 Hz in monkey LFP, whereas it ranged from 6 to 50 Hz in the human ECoG, suggesting that the corresponding frequency bands in the

monkey and human motor cortex might have shared functional roles. A further similarity of the present results from human recordings and previous results from monkey data pertains to the temporal evolution of decoding accuracy relative to the onset of the actual movement. In both monkey LFP (Mehring *et al* 2003) and human ECoG, a steep rise of DA was seen approximately 100 ms (monkey) and 200 ms (human) before movement onset, and a broad maximum in decoding accuracy was reached at roughly 150 ms after movement onset (single- and multi-unit activity from monkey), 250 ms (LFP from monkey) and at about 500 ms after movement onset (human ECoG recording from M1). The difference in the exact timing of DA changes might, at least in part, reflect the fact that monkeys moved faster (average movement durations of approximately 0.8 s versus 0.6 s in humans and monkeys, respectively), but it could also be due to the different signal types and/or recording locations used, or to functional differences between the human and monkey motor cortex.

The results discussed so far concerned decoding of four movement targets. We also analyzed data from an additional subject performing movements to eight targets. All principal findings from the four direction experiments were replicated in the case of eight directions. DA for eight directions was approximately 60%. Importantly, the confusion matrix for eight directions was clearly diagonally dominated, demonstrating that each direction could be discriminated from all other directions with reasonable accuracy, and that errors were mostly confined to immediately neighboring directions. Furthermore, many ECoG channels were cosine tuned in respect to arm reaching movement direction, both for the MRP and for gamma band amplitude modulations, in line with previous results that were obtained during continuous circular joystick movements (Schalk *et al* 2007).

As the movement task, we used natural center-out reaching movements. Reaching involves the action of many joints and muscle groups. The exact joint movements and their temporal sequence as well as the recruitment of the involved muscle groups may vary not only in different subjects but also within subjects as a function of movement direction. Therefore, some of the inter-individual differences observed in our study might be due to inter-individual differences in motor performance. Within subjects, directional differences might be related to the recruitment of different muscle groups or to different joint angles for the different reaching directions. The fact that reaching is a sequence of events may also explain movement direction-related response differences as shown in figures 9(a) and (b), as for instance differences in the timing of the contraction of a certain muscle group may be related in the observed differences in the timing of cortical motor responses for different movement directions.

Our study has implications for the development of a brain–machine interface for paralyzed patients. This idea has recently gained momentum by the demonstration, in rats and monkeys, that multiple single neuron activity can be employed to control an external actuator (Carmena *et al* 2003, Chapin *et al* 1999, Serruya *et al* 2002, Taylor *et al* 2002, Wessberg *et al* 2000); first findings in humans (Hochberg *et al* 2006) seem to point in a similar direction. In parallel, impressive progress has also been made in using the EEG recorded from the scalp surface for online movement control (Millán *et al* 2004, Wolpaw and McFarland 2004). There is, however, growing evidence from studies in monkeys and humans pointing toward the usefulness of neuronal population activity recorded with intracranially implanted electrodes, including both subdural and intracortical electrodes (Leuthardt *et al* 2004, Mehring *et al* 2003, Moritz *et al* 2008, Pesaran *et al* 2002, Rickert *et al* 2005, Rizzuto *et al* 2005, Schalk *et al* 2007, 2008, Velliste *et al* 2008). Our results, in fact, indicate that neuronal population activity from the human frontal lobe provides a potential basis for neuro-interfacing. Moreover, our results confirm that cortical neuronal population activity for movement inference can be reliably measured with electrodes placed on the brain surface, in contrast to previous models of BMIs using electrodes penetrating the brain tissue. Comparing the decoding accuracy of single channels of motor cortical human ECoG with monkey LFPs, however, we recently found that LFPs outperformed the ECoG significantly (Mehring *et al* 2004). On the other hand, there is also evidence suggesting that using denser electrode arrays, ECoG information yield might be increased considerably (Mehring *et al* in preparation).

Previously, we and others have proposed that recordings from more dense surface electrode arrays might also allow for individual finger control (Ball *et al* 2004). Furthermore, ECoG from the frontal cortex can also be used for the decoding of continuous movement trajectories (Pistohl *et al* 2008, Schalk *et al* 2007). Tkach and colleagues have shown that in monkey M1 and PM the modulation of spiking activity, its preferred directions and encoded information remained consistent during both movement observation and execution (Tkach *et al* 2007). A perspective for further investigations would be to study whether a similar principle also holds true for ECoG signals from the human M1 and PM regions.

The DA in our present study was in a similar range as that of four-target on-line cursor control reported in a recent ECoG study (Schalk *et al* 2008). This latter study used discrimination of different actual or imagined movement types for control of the two spatial dimensions, such as discrimination of imagined hand versus tongue movement. Therefore, population-signal-based BMIs in general, and ECoG-based solutions in particular, while being still in their infancy compared to EEG and single-unit activity-based approaches (e.g. McFarland *et al* 2008, Velliste *et al* 2008), must be considered as showing great potential for future development of BMIs for movement control. Moreover, our results provide valuable indications regarding the anatomical areas and signal frequency bands best suited for further research on the feasibility and usefulness of creating ECoG-based BMIs for interfacing the human cerebral cortex, especially for experiments using a closed-loop setup with real-time feedback of the controlled movement, where considerable improvements of performance might be achieved as compared to the closed-loop condition. Finally, the fact that we found significant information on arm movement direction also in premotor, prefrontal and parietal areas may be of considerable practical importance for BMIs as a new therapeutic option in the treatment of severely paralyzed patients in whom degenerative or ischemic lesion of the

primary motor cortex does not permit us to base data extraction on this area.

Acknowledgments

The WIN-Kolleg of the Heidelberg Academy of Sciences and Humanities and the German Federal Ministry of Education and Research (BMBF-DIP METACOMP and BMBF grant 01GQ0420 to the BCCN Freiburg) supported this project.

References

Andersen R A, Musallam S and Pesaran B 2004 Selecting the signals for a brain–machine interface *Curr. Opin. Neurobiol.* **14** 720–6

Aoki F, Fetz E E, Shupe L, Lettich E and Ojemann G A 1999 Increased gamma-range activity in human sensorimotor cortex during performance of visuomotor tasks *Clin. Neurophysiol.* **110** 524–37

Arroyo S, Lesser R P, Gordon B, Uematsu S, Jackson D and Webber R 1993 Functional significance of the mu rhythm of human cortex: an electrophysiologic study with subdural electrodes *Electroencephalogr. Clin. Neurophysiol.* **87** 76–87

Ball T, Demandt E, Mutschler I, Neitzel E, Mehring C, Vogt K, Aertsen A and Schulze-Bonhage A 2008 Movement related activity in the high gamma range of the human EEG *Neuroimage* **41** 302–10

Ball T, Kern M, Mutschler I, Aertsen A and Schulze-Bonhage A 2009 Signal quality of simultaneously recorded invasive and non-invasive EEG (submitted)

Ball T, Nawrot M P, Pistohl T, Aertsen A, Schulze-Bonhage A and Mehring C 2004 Towards an implantable brain–machine interface based on epicortical field potentials *Biomed. Tech. (Berlin)* **49** (Suppl. 2) 756–9

Ball T, Schreiber A, Feige B, Wagner M, Lucking C H and Kristeva-Feige R 1999 The role of higher order motor areas in voluntary movement as revealed by high-resolution EEG and fMRI *Neuroimage* **10** 682–94

Batista A P, Buneo C A, Snyder L H and Andersen R A 1999 Reach plans in eye-centered coordinates *Science* **285** 257–60

Birbaumer N, Ghanayim N, Hinterberger T, Iversen I, Kotchoubey B, Kubler A, Perelmouter J, Taub E and Flor H 1999 A spelling device for the paralysed *Nature* **398** 297–8

Brovelli A, Lachaux J P, Kahane P and Boussaoud D 2005 High gamma frequency oscillatory activity dissociates attention from intention in the human premotor cortex *Neuroimage* **28** 154–64

Carmena J M, Lebedev M A, Crist R E, O'Doherty J E, Santucci D M, Dimitrov D, Patil P G, Henriquez C S and Nicolelis M A 2003 Learning to control a brain–machine interface for reaching and grasping by primates *PLoS Biol.* **1** E42

Chapin J K, Moxon K A, Markowitz R S and Nicolelis M A 1999 Real-time control of a robot arm using simultaneously recorded neurons in the motor cortex *Nat. Neurosci.* **2** 664–70

Cheyne D, Bells S, Ferrari P, Gaetz W and Bostan A C 2008 Self-paced movements induce high-frequency gamma oscillations in primary motor cortex *Neuroimage* **42** 332–42

Connolly J D, Andersen R A and Goodale M A 2003 FMRI evidence for a 'parietal reach region' in the human brain *Exp. Brain Res.* **153** 140–5

Crone N E, Miglioretti D L, Gordon B and Lesser R P 1998a Functional mapping of human sensorimotor cortex with electrocorticographic spectral analysis: II. Event-related synchronization in the gamma band *Brain* **121** 2301–15

Crone N E, Miglioretti D L, Gordon B, Sieracki J M, Wilson M T, Uematsu S and Lesser R P 1998b Functional mapping of human sensorimotor cortex with electrocorticographic spectral analysis: I. Alpha and beta event-related desynchronization *Brain* **121** 2271–99

Dalal S S *et al* 2008 Five-dimensional neuroimaging: localization of the time-frequency dynamics of cortical activity *Neuroimage* **40** 1686–700

Dalal S S, Guggisberg A G, Edwards E, Sekihara K, Findlay A M, Canolty R T, Knight R T, Barbaro N M, Kirsch H E and Nagarajan S S 2007 Spatial localization of cortical time-frequency dynamics *Conf. Proc. IEEE Eng. Med. Biol. Soc.* vol 1 pp 4941–4

Efron B and Tibshirani R J 1998 *An Introduction to the Bootstrap* (London: Chapman and Hall/CRC)

Engel A K, Moll C K, Fried I and Ojemann G A 2005 Invasive recordings from the human brain: clinical insights and beyond *Nat. Rev. Neurosci.* **6** 35–47

Fernandez-Ruiz J, Goltz H C, DeSouza J F, Vilis T and Crawford J D 2007 Human parietal 'reach region' primarily encodes intrinsic visual direction, not extrinsic movement direction, in a visual motor dissociation task *Cereb. Cortex* **17** 2283–92

Fogassi L and Luppino G 2005 Motor functions of the parietal lobe *Curr. Opin. Neurobiol.* **15** 626–31

Friedman J H 1989 Regularized discriminant analysis *J. Am. Stat. Assoc.* **84** 165–75

Fuster J M 2000 Executive frontal functions *Exp. Brain Res.* **133** 66–70

Geyer S, Matelli M, Luppino G and Zilles K 2000 Functional neuroanatomy of the primate isocortical motor system *Anat. Embryol. (Berlin)* **202** 443–74

Hatsopoulos N, Joshi J and O'Leary J G 2004 Decoding continuous and discrete motor behaviors using motor and premotor cortical ensembles *J. Neurophysiol.* **92** 1165–74

Hochberg L R, Serruya M D, Friehs G M, Mukand J A, Saleh M, Caplan A H, Branner A, Chen D, Penn R D and Donoghue J P 2006 Neuronal ensemble control of prosthetic devices by a human with tetraplegia *Nature* **442** 164–71

Hoshi E and Tanji J 2004 Functional specialization in dorsal and ventral premotor areas *Prog. Brain Res.* **143** 507–11

Kornhuber H H and Deecke L 1965 Changes in the brain potential in voluntary movements and passive movements in man: readiness potential and reafferent potentials *Pflugers Arch. Gesamte Physiol. Menschen. Tiere.* **284** 1–17

Kovalev D, Spreer J, Honegger J, Zentner J, Schulze-Bonhage A and Huppertz H J 2005 Rapid and fully automated visualization of subdural electrodes in the presurgical evaluation of epilepsy patients *AJNR Am. J. Neuroradiol.* **26** 1078–83

Lachaux J P, Rudrauf D and Kahane P 2003 Intracranial EEG and human brain mapping *J. Physiol. (Paris)* **97** 613–28

Leuthardt E C, Miller K J, Schalk G, Rao R P and Ojemann J G 2006 Electrocorticography-based brain computer interface—the Seattle experience *IEEE Trans. Neural Syst. Rehabil. Eng.* **14** 194–8

Leuthardt E C, Schalk G, Wolpaw J R, Jemann J G and Oran D W 2004 A brain–computer interface using electrocorticographic signals in humans *J. Neural Eng.* **1** 63–71

Levine S P, Huggins J E, BeMent S L, Kushwaha R K, Schuh L A, Rohde M M, Passaro E A, Ross D A, Elisevich K V and Smith B J 2000 A direct brain interface based on event-related potentials *IEEE Trans. Rehabil. Eng.* **8** 180–5

McFarland D J, Sarnacki W A and Wolpaw J 2008 Electroencephalographic (EEG) control of three-dimensional movement *J. Neural Eng.* **5** 101–10

Medendorp W P, Goltz H C, Vilis T and Crawford J D 2003 Gaze-centered updating of visual space in human parietal cortex *J. Neurosci.* **23** 6209–14

Mehring C, Nawrot M P, Cardoso de Oliveira S, Vaadia E, Schulze-Bonhage A, Aertsen A and Ball T 2004 Comparing information about arm movement direction in single channels of local and epicortical field potentials from monkey and human motor cortex *J. Physiol. (Paris)* **98** 498–506

Mehring C, Rickert J, Vaadia E, Cardosa D O, Aertsen A and Rotter S 2003 Inference of hand movements from local field potentials in monkey motor cortex *Nat. Neurosci.* **6** 1253–4

Millán J, Renkens F, Mourino J and Gerstner W 2004 Noninvasive brain-actuated control of a mobile robot by human EEG *IEEE Trans. Biomed. Eng.* **51** 1026–33

Miller K J, Leuthardt E C, Schalk G, Rao R P, Anderson N R, Moran D W, Miller J W and Ojemann J G 2007 Spectral changes in cortical surface potentials during motor movement *J. Neurosci.* **27** 2424–32

Miller K J, Shenoy P, den Nijs M, Sorensen L B, Rao R N and Ojemann J G 2008 Beyond the gamma band: the role of high-frequency features in movement classification *IEEE Trans. Biomed. Eng.* **55** 1634–7

Moritz C T, Perlmutter S I and Fetz E E 2008 Direct control of paralysed muscles by cortical neurons *Nature* **456** 639–42

Musallam S, Corneil B D, Greger B, Scherberger H and Andersen R A 2004 Cognitive control signals for neural prosthetics *Science* **305** 258–62

Nair D R, Burgess R, McIntyre C C and Luders H 2008 Chronic subdural electrodes in the management of epilepsy *Clin. Neurophysiol.* **119** 11–28

Oldfield R C 1971 The assessment and analysis of handedness: the Edinburgh inventory *Neuropsychologia* **9** 97–113

Percival D B and Walden W T 1993 *Spectral Analysis for Physical Applications: Multitaper and Conventional Univariate Techniques* (Cambridge: Cambridge University Press)

Pesaran B, Nelson M J and Andersen R A 2006 Dorsal premotor neurons encode the relative position of the hand, eye, and goal during reach planning *Neuron* **51** 125–34

Pesaran B, Nelson M J and Andersen R A 2008 Free choice activates a decision circuit between frontal and parietal cortex *Nature* **453** 406–9

Pesaran B, Pezaris J S, Sahani M, Mitra P P and Andersen R A 2002 Temporal structure in neuronal activity during working memory in macaque parietal cortex *Nat. Neurosci.* **5** 805–11

Pfurtscheller G, Flotzinger D, Pregenzer M, Wolpaw J R and McFarland D 1995 EEG-based brain computer interface (BCI). Search for optimal electrode positions and frequency components *Med. Prog. Technol.* **21** 111–21

Pfurtscheller G, Graimann B, Huggins J E, Levine S P and Schuh L A 2003 Spatiotemporal patterns of beta desynchronization and gamma synchronization in corticographic data during self-paced movement *Clin. Neurophysiol.* **114** 1226–36

Pfurtscheller G and Lopes da Silva F H 1999 Event-related EEG/MEG synchronization and desynchronization: basic principles *Clin. Neurophysiol.* **110** 1842–57

Pistohl T, Ball T, Schulze-Bonhage A, Aertsen A and Mehring C 2008 Prediction of arm movement trajectories from ECoG-recordings in humans *J. Neurosci. Methods* **167** 105–14

Rickert J, Oliveira S C, Vaadia E, Aertsen A, Rotter S and Mehring C 2005 Encoding of movement direction in different frequency ranges of motor cortical local field potentials *J. Neurosci.* **25** 8815–24

Rizzuto D S, Mamelak A N, Sutherling W W, Fineman I and Andersen R A 2005 Spatial selectivity in human ventrolateral prefrontal cortex *Nat. Neurosci.* **8** 415–7

Rumeau C, Tzourio N, Murayama N, Peretti-Viton P, Levrier O, Joliot M, Mazoyer B and Salamon G 1994 Location of hand function in the sensorimotor cortex: MR and functional correlation *AJNR Am. J. Neuroradiol.* **15** 567–72

Santucci D M, Kralik J D, Lebedev M A and Nicolelis M A 2005 Frontal and parietal cortical ensembles predict single-trial muscle activity during reaching movements in primates *Eur. J. Neurosci.* **22** 1529–40

Schalk G, Kubánek J, Miller K, Anderson N, Leuthardt E C, Ojemann J, Limbrick D, Moran D, Gerhardt L and Wolpaw J 2007 Decoding two-dimensional movement trajectories using electrocorticographic signals in humans *J. Neural Eng.* **4** 264–75

Schalk G, Miller K J, Anderson N R, Wilson J A, Smyth M D, Ojemann J G, Moran D W, Wolpaw J R and Leuthardt E C 2008 Two-dimensional movement control using electrocorticographic signals in humans *J. Neural Eng.* **5** 75–84

Scherberger H and Andersen R A 2007 Target selection signals for arm reaching in the posterior parietal cortex *J. Neurosci.* **27** 2001–12

Schulze-Bonhage A H, Huppertz H J, Comeau R M, Honegger J B, Spreer J M and Zentner J K 2002 Visualization of subdural strip and grid electrodes using curvilinear reformatting of 3D MR imaging data sets *AJNR Am. J. Neuroradiol.* **23** 400–3

Schwartz A B, Moran D W and Reina G A 2004 Differential representation of perception and action in the frontal cortex *Science* **303** 380–3

Serruya M D, Hatsopoulos N G, Paninski L, Fellows M R and Donoghue J P 2002 Instant neural control of a movement signal *Nature* **416** 141–2

Shenoy K V, Meeker D, Cao S, Kureshi S A, Pesaran B, Buneo C A, Batista A P, Mitra P P, Burdick J W and Andersen R A 2003 Neural prosthetic control signals from plan activity *Neuroreport* **14** 591–6

Shenoy P, Miller K J, Ojemann J G and Rao R P 2008 Generalized features for electrocorticographic BCIs *IEEE Trans. Biomed. Eng.* **55** 273–80

Shibasaki H and Hallett M 2006 What is the Bereitschaftspotential? *Clin. Neurophysiol.* **117** 2341–56

Sinai A, Bowers C W, Crainiceanu C M, Boatman D, Gordon B, Lesser R P, Lenz F A and Crone N E 2005 Electrocorticographic high gamma activity versus electrical cortical stimulation mapping of naming *Brain* **128** 1556–70

Stark E and Abeles M 2007 Predicting movement from multiunit activity *J. Neurosci.* **27** 8387–94

Steinmetz H, Furst G and Meyer B U 1989 Craniocerebral topography within the international 10–20 system *Electroencephalogr. Clin. Neurophysiol.* **72** 499–506

Stepniewska I, Preuss T M and Kaas J H 1993 Architectonics, somatotopic organization, and ipsilateral cortical connections of the primary motor area (M1) of owl monkeys *J. Comp. Neurol.* **330** 238–71

Tanji K, Suzuki K, Delorme A, Shamoto H and Nakasato N 2005 High-frequency gamma-band activity in the basal temporal cortex during picture-naming and lexical-decision tasks *J. Neurosci.* **25** 3287–93

Taylor D M, Tillery S I and Schwartz A B 2002 Direct cortical control of 3D neuroprosthetic devices *Science* **296** 1829–32

Tecchio F, Zappasodi F, Porcaro C, Barbati G, Assenza G, Salustri C and Rossini P M 2008 High-gamma band activity of primary hand cortical areas: a sensorimotor feedback efficiency index *Neuroimage* **40** 256–64

Tkach D, Reimer J and Hatsopoulos N G 2007 Congruent activity during action and action observation in motor cortex *J. Neurosci.* **27** 13241–50

Toro C, Cox C, Friehs G, Ojakangas C, Maxwell R, Gates J R, Gumnit R J and Ebner T J 1994 8–12 Hz rhythmic oscillations in human motor cortex during two-dimensional arm movements: evidence for representation of kinematic parameters *Electroencephalogr. Clin. Neurophysiol.* **93** 390–403

Velliste M, Perel S, Spalding M C, Whitford A S and Schwartz A B 2008 Cortical control of a prosthetic arm for self-feeding *Nature* **453** 1098–101

Waldert S, Preissl H, Demandt E, Braun C, Birbaumer N, Aertsen A and Mehring C 2008 Hand movement direction decoded from MEG and EEG *J. Neurosci.* **28** 1000–8

Wessberg J, Stambaugh C R, Kralik J D, Beck P D, Laubach M, Chapin J K, Kim J, Biggs S J, Srinivasan M A and Nicolelis M A 2000 Real-time prediction of hand trajectory by ensembles of cortical neurons in primates *Nature* **408** 361–5

Wilson J A, Felton E A, Garell P C, Schalk G and Williams J C 2006 ECoG factors underlying multimodal control of a brain–computer interface *IEEE Trans. Neural Syst. Rehabil. Eng.* **14** 246–50

Wisneski K J, Anderson N, Schalk G, Smyth M, Moran D and Leuthardt E C 2008 Unique cortical physiology associated with ipsilateral hand movements and neuroprosthetic implications *Stroke* **39** 3351–9

Wolpaw J R and McFarland D J 2004 Control of a two-dimensional movement signal by a noninvasive brain–computer interface in humans *Proc. Natl Acad. Sci. USA* **101** 17849–54

Yousry T A, Schmid U D, Alkadhi H, Schmidt D, Peraud A, Buettner A and Winkler P 1997 Localization of the motor hand area to a knob on the precentral gyrus. A new landmark. *Brain* **120** 141–57